



A perspective for magic angle spinning above 250 kHz — OptiMAS

Jan G. Korvink¹

¹Institute of Microstructure Technology, Karlsruhe Institute of Technology, Hermann-von-Helmholtz-Platz 1, 76344 Eggenstein-Leopoldshafen, Germany

Correspondence: Jan G. Korvink (jan.korvink@kit.edu)

Abstract. Magic angle spinning averages out the dipolar coupling among spins in rigid solids, as well as other sources of magnetic inhomogeneity, leading to sideband suppression. To achieve line widths close to that achievable for the liquid state, it has been postulated that 250 kHz rotation frequencies have to be exceeded. Here we explore a perspective for a research project to achieve this goal.

Introduction

The solid state NMR (ssNMR) research field was initiated by the seminal papers of Andrew et al. (1958) and Lowe (1959) in the late 1950's. In this technique, a small molecular sample is spun at the magic angle of 54.73° with respect to the polarising magnetic field to achieve motional averaging of the solid's spatially constrained dipole-dipole spin interactions. ssNMR has become one of the most important experimental techniques with which to determine the structure of large proteins, delivering input required for deciphering the molecular nanomachinery of the cell.

Careful optimization of the stator and rotors have now reached an upper speed limit Schledorn et al. (2020) of 150 kHz, with rotor sizes down to 0.5 mm. Yet to the present day, commercial magic angle spinning (MAS) technology has remained essentially similar to the first scientific reports: a sample is packed into a rotor equipped with turbine blades, and driven into fast rotation by a pressurised gas stream. There is consensus in the ssNMR community that even higher sample rotation speeds Böckmann et al. (2015), operated within the highest feasible magnetic fields, and combined with dynamic nuclear polarisation, will not only provide the necessary improvements to overcome current day spectroscopic limitations, but will also allow new spectroscopic discoveries to be made Deschamps (2014).

The **OptiMAS**¹ concept was proposed to take this important groundbreaking step. It aims to establish the necessary modelling tools, and micro- and nano-engineering processes, to implement a new means to achieve significantly faster MAS rotation speeds whilst performing nuclear magnetic resonance with high signal-to-noise ratio. The high-risk-high-gain experimental route taken, based on the extensive use of light, was introduced to offer the opportunity to simultaneously cool the sample to cryogenic temperatures, and to generate dynamic nuclear polarisation within the sample volume.

¹The OptiMAS proposal was originally submitted to the European Research Council in 2017 but was not selected for funding.



The **OptiMAS** concept aims open up a window on research opportunities for high resolution solid state NMR, and if successful, would significantly extend the application range of high resolution MAS applied to fully protonated large protein molecules.

State-of-the-art

Section a. Biomolecular NMR.

Solid state nuclear magnetic resonance plays a key role in the structural elucidation of biomolecules, and aids in explaining molecular function Oschkinat et al. (1994); Deschamps (2014); Böckmann et al. (2015). Typical experimental procedures harvest target proteins that are expressed in bacterium cultures, which are then purified and isolated as small crystalline samples, packed by extended ultracentrifugation into magic angle spinner rotors, to be subsequently spun for NMR detection at high magnetic fields Böckmann et al. (2015). A major challenge is posed by the strong homonuclear dipolar interactions that occur in densely proton-populated regions of a molecule, leading to broad proton resonances at spinning speeds below 60 kHz. In order to partially suppress the anisotropic dipolar interactions that lead to unwanted broad resonance lines, rotation rates must at least exceed the size of the dipolar coupling linewidth Maricq and Waugh (1979), which for high- γ nuclei can be in excess of 100 kHz, otherwise spinning sidebands, separated at the rate of spinning, will overlap with the already crowded central spectrum Deschamps (2014); Böckmann et al. (2015). The combined challenges result in slow progress McDermott (2009):

”Although small globular proteins can be assigned with less than a year’s effort, larger more complex systems still tend to be a major undertaking.”

A strategy has been deuteration followed by 100 % reprotonation at exchangeable sites, but this severely limits observations of side-chain signals, and fractional ^2H labelling is only a partial remedy due to loss of sensitivity and resolution Andreas et al. (2016). Sample dilution through deuteration also does not help in dense contact cases where heteronuclear dipolar interactions are prevalent, or large anisotropic chemical shielding effects act, working against signal-to-noise ratio (SNR), and is questionable when unfolding is required Böckmann et al. (2015).

For large biomolecules, the inherent insensitivity of NMR leaves proton detection as the most straightforward means to gain sufficient signal from a molecular sample within reasonable experimentation time Andreas et al. (2016). Cross polarization Pines et al. (1972) is therefore one of the most important spectroscopic techniques, whereby coupling interactions are exploited to transfer polarisation from abundant spins I to the naturally dilute spins S (e.g., $I \in \{^1\text{H}, ^{19}\text{F}\}$ and $S \in \{^{13}\text{C}, ^{15}\text{N}\}$), and motional fluctuations of the field benefit the rapid transfer relaxation processes, but the technique only works if the rate of spinning is less than the anisotropic interaction. Efficiency of transfer depends on the Hartmann-Hahn condition ($\gamma_S B_{1(S)} = \gamma_I B_{1(I)}$) being well matched.

It is therefore only since the commercial announcement of 110 kHz MAS probeheads in 2013 Nishiyama et al. (2013) that it has become generally possible to consider fully protonated samples, with the first successful assignment reported recently

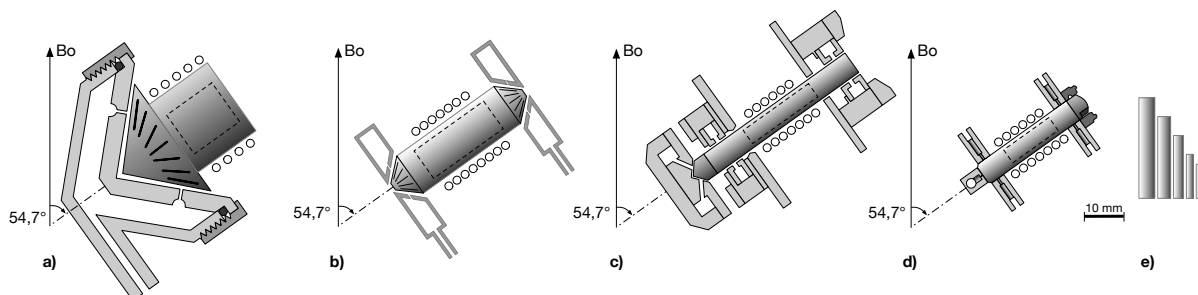


Fig. 1. Magic angle spinners are oriented at 54.7° to the polarizing field B_0 . **a.** Henriot Huguenard spinner. **b.** Double conical spinner. **c.** Modern single cone design. **d.** Modern Pelton turbine design. **e.** Five rotor sizes, currently available for the stator designs of **c**, **d**, are schematically shown: 4 mm, 3.2 mm, 2.5 mm, 1.3 mm, and 0.7 mm. Figures are approximately to scale, adapted from Andrew et al. (1958, 1969); Ackerman et al. (1979); Balimann et al. (1980); Eckman et al. (1980).

55 Andreas et al. (2016) for a 28 kDa protein inside a 2.5 MDa viral capsid.² To quote Andreas et al. (2016) on the advantages of faster 100 kHz MAS:

”...nonexchangeable protons lie in the most structured regions of a protein, where the density of potential internuclear contacts is higher. The possibility of studying samples directly expressed in 100% H_2O is an advancement that extends 1H -detected structural determinations to key exchange-protected regions.”

60 whereas Böckmann et al. (2015) state that:

”... many NMR experiments are best performed at MAS frequencies as high as possible ... We extrapolated that around 250 kHz, fully protonated proteins will lead to lines comparable to the ones presently obtained from deuterated and fully back-protonated systems at 100 kHz ... Fast MAS, faster than 100 kHz, seems to open the way for protein analysis and structure determination with sub-milligram amounts of protein.”

65 Section b. Ultrafast magic angle spinning.

The Henriot Huguenard spinner depicted Fig. 1a, inspired by advances in centrifuge design, dominated early NMR experiments from 1958 to 1979 Andrew et al. (1958, 1969); Ackerman et al. (1979), and had a rotation rate limit at 10 kHz. Higher speeds and flexible experimentation necessitated more stable gas bearings Balimann et al. (1980), and some versions combined axial and radial supports Eckman et al. (1980), also see Fig. 1b. State-of-the-art gas turbines separate drive and support (see Fig. 1c &
 70 1d), and require high precision design to reach the current record speeds of up to 120 kHz. These represent the fastest rotating devices available commercially, unsurpassed even by ultracentrifugation equipment, which currently reach up to 2.5 kHz.

Despite very impressive recent advances, current gas turbine MAS technology is not scalable to overcome its limitations Wilhelm et al. (2015), and hence the research roadmap should be reconsidered. The kinetics of fast rotation demand rotor

²Fast spinning also enhances the $^1H T_2'$ relaxation time, and decouples $^1H^{14}N$ interactions, and through use of microcoils with stronger ^{14}N radiofrequency fields and higher detection sensitivity, lead to significant resolution enhancement Nishiyama et al. (2011); Böckmann et al. (2015).



diameters of 100 μm and less³, and highest mechanical strength. A picolitre of homogeneous sample volume at low filling factor would yield NMR signal intensities close to the Faraday limit-of-detection. Gas turbine based momentum transfer to the rotor increasingly results in frictional drag, causing sample heating. Sample sizes are small relative to microwave wavelengths, making power absorption challenging. On the positive side, there is no NMR evidence that fast rotation affects protein crystal structure or molecular assemblies significantly Böckmann et al. (2015).

A number of alternative microsystem concepts have been reported to achieve small rotational drives. Induction based micromotors Büttgenbach (2014); Poletkin et al. (2016) are precluded from use with MAS, because unshielded varying magnetic fields cause by a $\mathbf{j} \times \mathbf{B}_0$ modulation required for torque generation would disturb the NMR experiment due to periodic variation of the chemical shift. Variable reluctance micromotors would simply not work due to saturation of the flux guiding soft-magnetic materials at around 1.5 T. Commercially available brushless micromotors achieve highest reported rotation rates of up to 20 kHz Maxon (2015).

Electrostatic motors have highly localised strong electric fields which would not directly disturb the magnetic field, but are susceptible to dust accumulation, and require very narrow gap tolerances of a few tens of μm in order to generate enough torque Zhang et al. (2005). Current challenges include electrostatic discharges over the small gaps, and support friction, both of which hamper both operation and reliability Zhang et al. (2005). Also, the numerous electrodes would disturb NMR detection. Piezoelectric drives are magnetic field compatible can achieve very high frequencies, but rotation drives require friction which limits rotation rates to 200 Hz Newscaletech (2015).

The fastest reported rotation rate of 5 MHz has been achieved by angular momentum transfer from a circularly polarized optical beam to an optically trapped 4.4 μm diameter uniaxially birefringent vaterite particle, performed at a pressure of 0.1 Pa to reduce drag resistance Arita et al. (2013). Notably, the trap conditions stabilise under the action of rotation. The key idea rests in transfer of orbital angular momentum (OAM), imprinted through a helical phase distribution about the propagation axis, of a suitably prepared vortex beam of coherent light. The OAM of a beam can in principle be multiple times the photon spin Padgett and Bowman (2011). Apart from through helical phase distributions, a light beam can also generate torque in a levitated particle through inherent birefringence of the particle, by suitable light scattering from the object, asymmetry in the beam shape acting on an asymmetric particle, and by using the shape of the particle to generate an OAM scattered field from non-prepared light Padgett and Bowman (2011). Reflecting 25 years of research in orbital angular momentum, Padgett (2017) recently summarized:

”... the realisation that the Poynting vector can be engineered over the beam cross-section has triggered research into many beam types, and light-matter interactions in both the classical and quantum regimes ... enable new applications in imaging, sensing and communications.”

³Due to material strength limitations, $\nu \cdot D = (3/\pi) \sqrt{T\Delta/\rho} \approx 90 \text{ Hz m}$, where D is the MAS rotor diameter in m, ν the rotation rate in Hz, T is the tensile strength of the rotor in Pa, Δ the relative wall thickness of the rotor, and ρ the density of the rotor in kgm^{-3} Samoson et al. (2004).

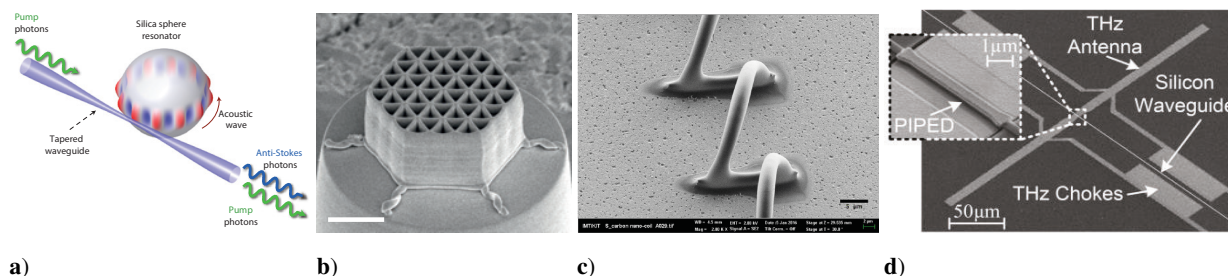


Fig. 2. State-of-the-art: **a.** Brillouin cooling of a $77.5\,\mu\text{m}$ silica microsphere Bahl et al. (2012). **b.** Highest strength-to-density ratio nano-material Bauer et al. (2016). Scale bar: $2\,\mu\text{m}$. **c.** Nanostructured and pyrolysed photopolymer precursor achieves shape and allotrope Sharma et al. (2016). Scale bar: $5\,\mu\text{m}$. **d.** Direct opto-electrical signal conversion Melikyan, A et al. (2014); Harter et al. (2016). Scale bar: $50\,\mu\text{m}$. All figures were extracted and adapted from the cited papers.

Section c. Cooling.

For magic angle spinning, current practise for sample cooling is to use cooled driving gases (nitrogen or helium), a procedure that works down to cryogenic temperatures, and is regularly applied in DNP-MAS Barnes et al. (2008). When gases are no longer used to drive rotation, and the gas pressure is drastically reduced to reduce friction, this method is no longer efficient, and cannot compensate other sources of heating.

In 1929 the physicist Peter Pringsheim proposed that light could be used for cooling Pringsheim (1929). Whereas it is well known that atoms and molecules can be cooled by light Diedrich et al. (1989), it was only in 1995 that a solid was cooled to $110\,\text{K}$ by laser-induced fluorescence Epstein et al. (1995). In 2011 a macroscopic $10\,\mu\text{m}$ micrometre object was cooled into its ground state by optical cavity back-action Chan et al. (2011). A phononic bandgap shield for bulk phonon modes isolated a nanobeam from the silicon chip support, which contained a periodic structure to localise the phononic and photonic modes to the beam centre. The electrostrictive effect can also be exploited to achieve Brillouin cooling, by creating separate Stokes and anti-Stokes optical resonances differing by the mechanical resonance of $95\,\text{MHz}$, and using the latter resonance for emission Bahl et al. (2012). By using azimuthal whispering gallery modes of optical propagation along the device equator avoids dissipation at anchoring sites, achieved a mode temperature of $19\,\text{K}$ for a $77.5\,\mu\text{m}$ SiO_2 sphere in a room temperature experiment.

In a recent comprehensive review of the large number of reported optomechanical cooling mechanisms Yong-Chun et al. (2013), the authors encourage focusing research on applications:

... These schemes add complexity to the current experimental systems, and thus efforts should be taken to demonstrate these schemes in real experiments, which would be possible in the near future.



Section d. Nanotechnology for novel materials and high strength-density ratios.

Currently, high speed MAS rotors are made of stabilised zirconia (ZrO_2), aluminium nitride (Al_3N_4), or sapphire (Al_2O_3). Rotor caps are made of the ceramics ZrO_2 , Macor, boron nitride (BN), or the polymers Vespel and Kel-F. The key performance factor is a high tensile strength T to density ρ ratio $\sqrt{T/\rho}$, typically between 300 ms^{-1} to 400 ms^{-1} . Recently, an artificial metamaterial was reported exhibiting $\sqrt{T/\rho} = 2000 \text{ ms}^{-1}$. The pure glassy carbon nanomaterial, in a honeycomb arrangement, was made by two photon polymerisation of a photoresist precursor followed by pyrolysis Bauer et al. (2016). Nano-pyrolysis can control the carbon allotrope Sharma et al. (2016). Because of the low density due to its porous structure, the effective ^{13}C concentration can be diluted by a factor of 2.5 below bulk (0.44%), so that low NMR background signals are to be expected.

130 Section e. Signal generation.

The drive in mobile communications, built upon continued advances in miniaturization, as well as device and system innovations, has not only allowed the semiconductor industry to keep up with the Moore's law prediction for shrinking chip size, but also to keep raising the frequency of solid state devices, so that currently multiple GHz chipsets are commercially available.

NMR spectrometer electronics may become more compact, as exemplified by open source software-defined-radio projects Tang and Wang (2011), in contrast to high power commercial systems. Recent advances in nanodevices Melikyan, A et al. (2014); Harter et al. (2016) are paving the way to achieve record high speed signal processing using electro-optical modulators. In a device that measures only $29 \mu\text{m}$ in length, electro-optical phase modulation of an infrared light beam was demonstrated up to 40 Gbits^{-1} Melikyan, A et al. (2014), based on surface plasmon polariton excitation in a metallic-nanogap travelling wave modulator, surrounding an optical waveguide displaying the Pockels effect.

140 The situation is similar for microwave frequencies in the dynamic nuclear polarisation range 9 GHz to 600 GHz. Macroscopically sized gyrotrons and klystrons remain the best choice for powers of 5 W and above. They are available from NMR vendors in frequencies up to 527 GHz, for 25 kHz MAS rates of 1.9 mm rotors cooled to 100 K. Solid state sources are now available up to 1.1 THz at low power. To generate and detect up to THz radiation, a photomixer was reported that employs a tapered silicon waveguide clad with adjacent Au and Ti electrodes that form a plasmonic internal emission detector (PIPED) Harter et al. 145 (2016). The resulting high frequency current was coupled to an antenna, with frequency dependent powers ranging between -60 dBm to -80 dBm .

Section f. Signal enhancement for Faraday NMR detection.

The most obvious way to enhance the NMR signal-to-noise ratio is through coil miniaturization Olson et al. (1995). The record limit of NMR detection by Faraday induction is $0.36 \text{ nmol s}^{1/2}$ of a 4 pL voxel, with a linewidth of 1.7 ppm in an imaging experiment Ciobanu and Pennington (2004). A comprehensive comparison of miniaturized detectors is given by the review Badilita et al. (2012b). Spectroscopic quality microdetectors are typically implementations of striplines Bart et al. (2009), saddle coils Wang et al. (2017), or Helmholtz coils Spengler et al. (2016), where radiofrequency resistance sets the technical limit of

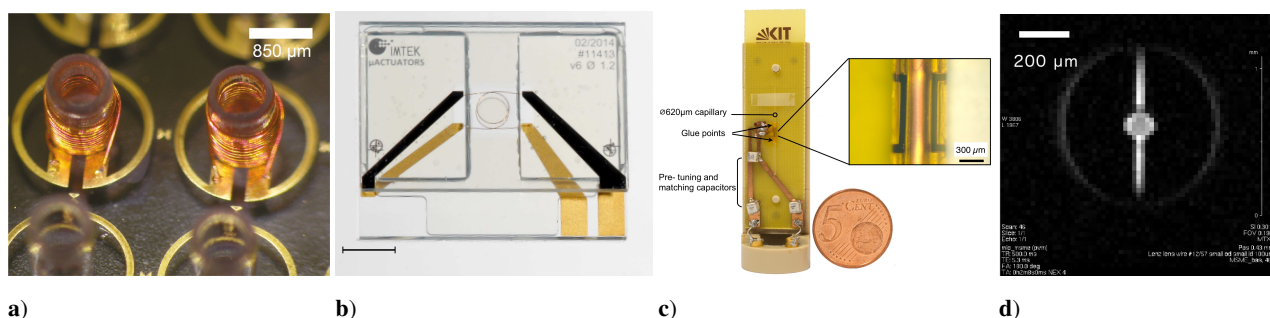


Fig. 3. Faraday detection NMR microsystems. **a.** Magic angle coil spinning (MACS) microsystem Adhikari et al. (2017). Scale bar 850 μm . **b.** Helmholtz solenoidal microcoil with 113 nL sample volume and 0.6 Hz intrinsic linewidth Spengler et al. (2016). Scale bar 2 mm. **c.** Saddle coil with 650 μm capillary Wang et al. (2017). Insert scale bar 300 μm . **d.** Microscale Lenz lens focuses flux from 1 mm to 100 μm Spengler et al. (2017). Scale bar 200 μm . All figures were extracted and adapted from the cited papers.

miniaturization to 50 nL to 100 nL sample volumes. To increase detector signal-to-noise ratio for smaller volumes requires a Lenz lens flux transformer Spengler et al. (2017); Meier et al. (2017).

155 For further signal enhancement, either a hypersensitive detector, or a hyperpolarisation method, must be used. For example, dynamic nuclear polarisation exploits the high electron gyromagnetic ratio to transfer polarisation from sample electrons to protons Abragam and Goldman (1978), and the typical way to perform high field DNP is by microwave irradiation, of a glassy sample suitably doped by radicals and rapidly cooled down to 90 K, at the electron resonance frequency Barnes et al. (2008). Room temperature DNP enhancement of ^{13}C to levels up to 6%, representing an enhancement of around 170 000, has been
 160 achieved through the optical pumping of the nitrogen vacancy (NV) in diamond, under thermal mixing of the dipolar coupling to nearby nuclei, and and through simultaneous microwave driven electron/nuclear spin flips to drive the solid effect King et al. (2015). The same NV centres could also be used for NMR detection readout. It has been shown that NV fluorescence remains stable up 10 T field strength Stepanov et al. (2015).

Section g. Concluding remarks

165 This compact literature review reveals that the limits of current MAS technology may be overcome by a coordinated use of light as a solid state NMR tool. This represents the central concept of the **OptiMAS** proposal, for which the research approach is now discussed.

Research objectives

The overall objective of **OptiMAS** is to achieve a completely new tool for solid state NMR spectroscopy, by systematically
 170 addressing the major technical challenges facing the analysis of large biomolecules through a micro and nano engineering approach, see Fig. 4. In our concept, light will become the primary workforce with which to suspend, rotate, and cool the sample,

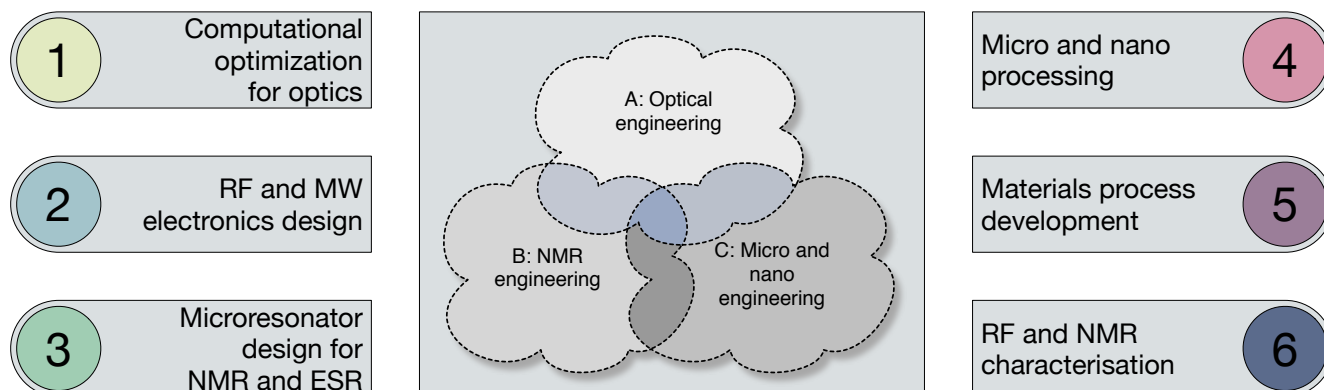


Fig. 4. The **OptiMAS** proposal addresses the micro and nano engineering challenges that arise at the intersection of optics and photonics, micro and nano processing, and high resolution NMR detection, indicated by the six numbered topics .

and to manipulate its spins. We aim to achieve these functions first separately, then in combination, and place them under the control of typical spectrometer software. Several research aspects arising from the the state-of-the-art have been identified that need to be solved to make this desirable technique available to a broad community of researchers from solid state bio-NMR. We first consider those research objectives (**ROs**) that directly relate to magic angle spinning:

RO-1: Ultrafast magic angle spinning. MAS spinning rates are required that significantly overcome the current speed record of 120 kHz by a factor of 2 to 6, principally to provide a tool for the removal of homonuclear line broadening due to close-proximity ($<1 \text{ \AA}$) protons in dense fully-protonated molecular networks, to result in solution-like spectra. High speeds will also benefit decoupling procedures, by increasing the number of polarisation transfers that can be performed. Isotropic mixing will also become more efficient, thereby avoiding the use of high excitation field powers, which will also reduce radiofrequency sample heating. Fast rotation will require precisely micro-manufactured rotors with rotor diameters below $100 \text{ }\mu\text{m}$, containing $<1 \text{ nL}$ of sample. Rotation must take place within the confinement of a high signal-to-noise ratio, narrow linewidth NMR detection device, see **RO-4** below. Surface friction on the rotor must be reduced by operation in a vacuum of $<1 \text{ Pa}$.

RO-2: Facile sample preparation and handling. A completely new concept is required for tiny MAS rotors and their handling during sample preparation and loading into the MAS probehead. Rotors must offer strength and robustness against highest rotation rates of 250 kHz to 800 kHz, be precisely formed, and fulfil the primary requirements of optimal momentum transfer. New MAS sample packing procedures, also for centrifugation, must be developed that are compatible with isolation and purification steps. Rotor materials should not produce disturbing NMR background signals, hold a volume in the range of 5 pL to 10 pL and should additionally support cooling, signal detection, and signal enhancement procedures. Novel materials must be combined with micro and nanostructuring techniques to achieve mass producible solutions at reasonable effort.



RO-3: Sample volume cooling. Ultrafast rotation and spin excitation is likely to result in heating of the small sample, especially if operated in vacuum. Special provision should be made for continuous *in situ* monitoring of the sample's temperature without contamination. Closed loop cooling must be established to maintain constant and precise spectroscopic conditions to $<0.1^{\circ}\text{C}$ over weeks of experiment time. For samples containing water, the temperature should be maintained in the range 1°C to 10°C . The cooling range should be extended down to the 100 K regime to meet with DNP requirements.

Next we discuss the research objectives that relate to the complete NMR signal chain:

RO-4: High SNR detection path. Small sample sizes will deliver faint NMR signals that must be optimally collected for processing. Despite the small sizes involved, detector designs must maintain a high intrinsic signal-to-noise ratio, cause negligible susceptibility mismatch due to the high magnetic field, despite potential misalignment at the magic angle, and must not interfere with other procedures such as rotation, cooling, and microwaves.

RO-5: Microwave signal generation and deposition. For electron spin excitation and manipulation at high magnetic field, it will be necessary to supply microwaves in the sub-THz regime with sufficient power density and signal processing flexibility. Radiation must be deposited with a uniform intensity profile that largely overlaps with the sample volume. To guide the radiation optimally to the sample and condition it for effective absorption, microfabricated quasi-optical structures should be considered.

RO-6: Signal enhancement. Because of the small sample volume of $v \leq 10\text{ pL}$, non-equilibrium signal enhancement will be considered to avoid long signal averaging periods that would otherwise slow down acquisition.

Finally, we delineate the objective that deals with the research outcome as a spectroscopy tool.

RO-7: Modular ultra high speed MAS platform. In order to gain the most benefit from the preceding objectives, a platform is required that co-integrates sample insertion, levitation, rotation, cooling, excitation, and detection signal path into a tight package of high precision and reasonable cost, seamlessly into a narrow-bore NMR spectrometer. Apart from modularity, which will support experimentation and the management of multiple workpackages, and avoid the complete re-development of components should only part of the experiment require new capabilities, it will be essential to properly interface the probehead with a commercial spectrometer so as to benefit from the installed base and prior know-how. Such a platform must be extensively characterised using available NMR sequences (1D, 2D, 3D) to verify basic NMR function. It will also ensure that the approach is 'spectroscopist-friendly'.

Section a. Methodology

There is a strong need to improve both detection sensitivity and measurement throughput in structure elucidation. Despite the utility of the solid state NMR approach, and the tremendous recent advances in MAS and DNP instrumentation and associated methodology, the protein data bank (PDB) contains only 104 entries⁴ of structures elucidated by solid-state NMR over the past

⁴Size distribution: up to 10 kDa, 49 structures; up to 100 kDa, 43 structures; up to 1 MDa, 8 structures.

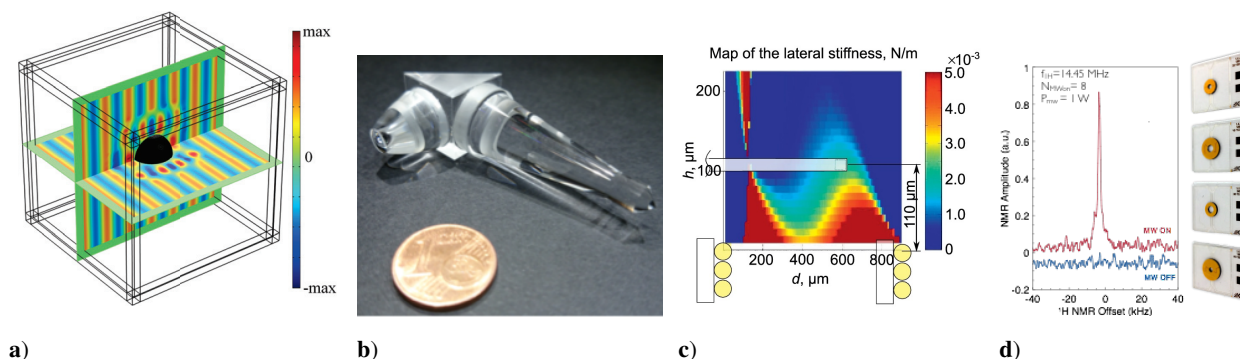


Fig. 5. Exemplary results from the author's group that underscore some of the arguments in this paper. **a.** Numerically optimized optical intensity profiles around a dielectric sphere Deng and Korvink (2016b). **b.** NMR-compatible double-axicon-based optical tweezers Kampmann et al. (2018). **c.** Stability model for stable suspension dynamics Poletkin et al. (2017). **d.** Overhauser-DNP microchips (right) and resulting Overhauser-DNP enhancement Kiss et al. (2021).

20 years PDB (2017). This stands in stark contrast to the number of important systems to study, and is an indication for the extraordinary experimental effort involved.

225 Whereas the development of experimental techniques for solid state NMR is firmly in the hand of spectroscopists, the implementation of novel and efficient experimental equipment *necessarily also requires an engineering approach*, even more so when sample sizes are small, signal levels are low, and when multiple technical disciplines are involved. To fulfil the various research objectives of **OptiMAS**, we would have to address the following engineering research challenges (**RCs**):

RC-1. Computational optimization of nanooptical elements (RO-1, RO-3, RO-5): Numerical optimization will be required to design required optical functional elements that are highly compact and repeatedly manufacturable. At the micro and nanoscale, there is a smaller choice of suitable processable materials, and manufacturing restrictions on geometries exist. Metamaterial-like geometries offer the potential to implement light-guiding functions compactly through the planar and volumetric arrangement of sub-wavelength diffractive and refractive nanostructures. Initial 2D numerical experiments show potential in predicting axi-symmetrical structures. Chiral structures in 3D are required to achieve light beams with optimal orbital angular momentum. A fully general 3D finite element implementation is still lacking (despite initial efforts Deng and Korvink (2016a)), and poses a major challenge to be solved.

OptiMAS would remove this deficiency by creating a 3D topology optimization design tool that allows the determination of nano-manufacturable diffractive and refractive optical elements. The tool would be used for numerous optical optimization tasks, including beam preparation for the optical tweezers' primary functions of levitation, which will require confected trap stiffness, and rotation. The tool would also be used to determine the layout of the MAS rotor for optimal transfer of orbital angular momentum by means of shape chirality. For cooling, the tool would be used to evolve a high finesse optical resonator with good optical coupling to the mechanical vibrational modes. Rotational dynamics would require know-how and computational capabilities in inductive levitation mechanics, see Poletkin et al. (2017).



RC-2. Optical levitation and spinning (RO-1, RO-7): For high resolution magic angle spinning, a suitably prepared sample must be suspended in a containing MAS rotor with sufficient force against gravity, and stably spun at high mechanical rates in the range 250 kHz to 800 kHz, and with known rotation phase. Furthermore, sample insertion into the spinner optical beam must be convenient, efficient, and repeatable. A number of technical issues must be carefully resolved: the measured rotation rate must be known to a high accuracy of <1 Hz, and at low latency, to form the jitter-free input to a closed loop torque control system that regulates the MAS rotation rate. Provision must be made to remove surface friction by surrounding gases at a partial vacuum of <0.1 Pa, so as to minimize frictional losses Geropp.

Tweezer optical elements, computed by the methods of **RC-1**, would be nano-manufactured by direct write nanolithography Deubel et al. (2004); Gissibl et al. (2016). The high numerical aperture optical elements would be designed to create a strong and stable 3D optical force field of >100 pN (also see **RC-3**), and to impart to its light beam a phase vortex of the highest possible index using a nanoscale phase mask. Laser light would be coupled into the trap optics via optical fibre. Microfabrication processes will be required to combine the tweezer optics with a small volume transparent vacuum chamber that facilitates sample loading and unloading, and simplifies the localisation of the sample relative to the tweezer's focal point. Built-in piezoelectrically-actuated shaking is proposed to agitate the small MAS rotor and thereby to move it into the trap. For these initial experiments, the rotor-sample would be a commercially available microparticle of a weight of at least 10 pg with known NMR signature. As soon as **RC-3** delivers first sample containers, all effort would continue with custom solutions. Modulations of the back-scattered light due to remaining optical inhomogeneities in the sample would be employed to extract the instantaneous rotation rate.

RC-3. Rotor sample holder (RO-2, RO-3, RO-5): The achievement of an opto-mechanical rotor forms a central challenge for **OptiMAS**. First and foremost, it must interact with the trapping beam to achieve stable highest levitation forces and rotational torque. The sample container must optimise these functions simultaneously, and in concert with the trap optical design. In order to raise optical levitation forces from typically tens of pN by one to two orders of magnitude, it will be essential to reduce optical absorption towards achieving pure optical scattering, and to precisely guide scattering forces to achieve maximum momentum transfer.

Our approach would be to use 3D direct write nanolithography to achieve highly efficient optical nanostructures that are topology optimized with the methods established in **RC-1** to achieve the required kinetic functions. In addition, the rotor must provide sufficient mechanical strength to resist the high centrifugal forces due to rotation above 120 kHz, and should provide provision for cooling, speed, and temperature monitoring functions.

Investigations on the use of multiple materials would be required to assist in achieving the various goals. For example, for mechanical strength, the use of thermally processed nanopatterned photoresists would be considered to achieve high porosity of the mechanical structures for high strength-to-weight ratios, yet retain hermiticity of the sample space, and leave room for optically transparent materials to implement the other optical functions. The rotor would be designed to withstand the stresses due to rotation rates in the range 250 kHz to 800 kHz. Thus, at a later stage in the project, the outer perimeter of the rotor would be envisaged to become an optomechanical resonator, through which opto-mechanical



cooling will be implemented. The optical beam for cooling must be well-isolated from other optical functions, and insertion structures should not interfere with momentum transfer. Already at an early stage in the project it would be necessary to consider the handling of the rotors, for sample filling, for insertion into the probehead, and for storage. For more details, see **RC-6**.

RC-4. Magic angle spinning and NMR detection (RO-1, RO-7): Upon achievement, this research challenge amounts to the first major milestone for **OptiMAS**. The optical trap, including vacuum enclosure and sample, must be operated within the confines of a microcoil detector, within the narrow bore of a strong NMR magnet. Whereas separate functions can be verified at the bench, only the detection of an NMR signal with rotation-dependent spinning sidebands will demonstrate the ultimate functioning of the setup. The achievement will also form the basis for all subsequent challenges.

It is envisaged to build upon prior results of the Helmholtz Spengler et al. (2016) or RUMS Wang et al. (2017) microcoils, perhaps including an additional Lenz lens Spengler et al. (2017) to achieve highest possible signal-to-noise ratio (depicted in Fig. 5b, 5c and 5d). The integration of a microcoil would include a four channel trap circuit to facilitate multi-dimensional NMR pulse sequences. The setup must be conceived not to disturb the optical trapping functions. It is envisaged that the project would also entail a large amount of characterisation, not only of the NMR detection functions, but also of robustness w.r.t. long detection periods (hours, days, weeks) and to 'blind' initiation within the bore of the magnet. Also, there will be a need to verify the ability to ramp the spinning speed, and the precision with which the speed can be monitored and controlled. The ability to accurately monitor the temperature, done most likely by incorporating temperature sensitive fluorophores in the rotor materials to obtain a unique signature, would need to be tested. Further characterisation of the increases in temperature during pure rotation, and during pulsing with variable bandwidths, would be needed to reveal the cooling requirements for **RC-5**.

RC-5. Sample cooling (RO-3, RO-4, RO-6): Multidimensional solid state NMR characterisation of small samples will require extended experimentation time, and maintaining stable temperatures within a small range during acquisition will be essential for spectral quality, avoiding unnecessary line broadening and sample degradation. Because of sample operation in partial vacuum to reduce frictional drag, temperature equilibration with the remaining surrounding gas will be inefficient. Dielectrically driven absorption of radiofrequency energy, and light, will therefore require special precautions to avoid the almost adiabatic heating of the sample.

Our approach would be to modify the rotor to additionally implement a high finesse opto-mechanical cavity, most likely in the form of a rotationally symmetric ring oscillator, and to optically drive aximuthal vibrational modes by heterodyne opto-mechanical coupling through the mixing of two relatively mistuned laser beams, to achieve resultant cooling of the rotor. The simulation capabilities resulting from **RC-6** would form an important basis for the required predictive design. The photonic temperature monitor established in **RC-4** would form the basis for characterisation.

RC-6. Establishment of an MAS workflow (RO-2, RO-7): The necessarily small picolitre-sized sample volume will be challengingly close to the lower limit of NMR inductive detection, which will require special procedures for handling. At



the same time, the rotor itself will also be inconveniently small, less than 100 μm in diameter and height, and prone to damage if manually handled. Provision must be made to insert the sample exactly in its sample space, avoid contact with any optical nano-structures, include a means to confirm successful filling, after which to transfer the sample assembly into the vacuum chamber for evacuation and subsequent insertion into the probehead.

315 The **OptiMAS** approach will be to build upon a cassette-like structure, established by micro structuring from NMR compatible materials. The cassette will render the rotor compatible with sample placement through ultra-centrifugation, microscopy, sample volume cleaning procedures, and will be "finger"-compatible for manual insertion operations. Internal structures will confine the rotor from falling out of the cassette. The cassette will snap into the miniaturized vacuum chamber, to approximately align with the axes of the optical tweezers for ease of trapping, for subsequent evacuation.

320 Rotors will easily insert into conventional MAS stators, in combination with magic angle coil spinning microcoils (MACS, see Badilita et al. (2012a)), which could be used to characterise the amount of filling, and the level of background signals.

RC-7. Electron spin resonance (RO-4, RO-5, RO-6, RO-7): The optical tweezers will suspend a 5 pL to 10 pL rotor containing around 10^{12} 1 kDa proteins⁵. For ^1H -NMR at 11.7 T, this volume is at the limit of detection of the currently best microcoil arrangement, leaving practically no leeway for direct detection of ^{13}C or ^{15}N . Although higher magnetic fields will help, signal enhancement strategies that achieve non-equilibrium polarisation, such as dynamic nuclear polarisation, must be considered.

325

Our novel approach would be to pursue one of the unique opportunities offered by the heterodyne mixing of two similar-wavelength laser beams, resulting in tunable optical beat frequencies spanning the entire electron spin resonance range 200 GHz to 658 GHz relevant for DNP in high fields ($B_0 \in 7\text{ T to } 23.48\text{ T}$). Interfering beams would be used to drive a plasmonic resonating nanoscale diode below its THz cutoff frequency, whose ps-scale modulated current is in turn driving a loop or reflection-mode near-field antenna directly surrounding the sample. Because these chip-based devices are potentially very small ($<1\text{ mm}$ overall), they could be operated in close proximity to the sample, to offer sufficient power density for saturated electron excitation of incorporated biradicals. Initial experiments would first focus on establishing a DNP capability, before being joined with the MAS capabilities.

330

335 **RC-8. Integration (RO-1, RO-2, RO-7):** The unique possibility to transfer three MAS procedures, namely suspension, rotation, and cooling, to an implementation based on laser beams intersecting within a sub-millimetre sample space, harbours the challenge that these procedures should not interfere, so that they can be operated simultaneously and in a coordinated fashion within an NMR experiment, ultimately enhanced by DNP. A considerable effort should therefore be invested in integration activities.

340 This central *engineering research challenge* would therefore address the modularity, interoperability and electrical control of all subsystems, and the integration of the capability into the MAS experimental workflow (**RC-6**). Our approach would be to develop a dedicated NMR probe-head that is plug-in-compatible with a commercial spectrometer system. Extensive

⁵Corresponding to a partial specific volume of $0.73\text{ cm}^3/\text{g}$, proteins occupy $1.212 \times 10^{-3}\text{ nm}^2/\text{Da}$ Erickson (2009).



light beam management would be performed, to minimize the number of required light sources. Extensive diagnostics would be implemented, to ease initiation of the measurement process, and verify correct operation.

345 **RC-9. Functional verification (RO-1 to RO-7):** The ultimate target of **OptiMAS** is to facilitate, from the solid state, liquid state equivalent ^1H spectra from large, fully protonated proteins. In order to arrive at this performance, all technical subsystems must properly cooperate and synchronise, and must deliver the designed performance values.

In order to verify the various functionalities, experiments with exemplary samples, obtained through existing cooperations, would be conducted that reveal the attained performance, such as enhancement of signal-to-noise ratio, sufficiency of spectral linewidth, instrumental stability during long experiments, and the ability to perform a wide spectrum of pulse sequences. Spectroscopy would be performed on these representative proteins to benchmark not only performance, but potentially reveal novel capabilities of the new instrumentation, such as enhanced isotropic mixing under low power input, increased numbers of polarization transfers, and the ability to resolve crowded sub-spectra from dense proton networks in challenging dimeric structures. In conjunction with DNP, one would aim to demonstrate a strong reduction in experiment time.

350

355

Conclusions

As delineated, increased spinning rates for solid state NMR samples implies the use of smaller sample radii, to overcome yield-strength limitations and achieve rotation rates above 150 kHz. In turn, smaller sample sizes will lead to lower NMR signal levels, necessitating the use of a hyperpolarisation technique. Together with cooling, all three techniques could benefit from operation inside an optical trap. The trap would be located within the bore of a high field magnet, embedding the sample within a suitable microcoil or other sensitive detector. The basic concepts for these steps are already available, in principle, and a suitable research programme could bring them all into suitable concert.

360

Author contributions. This is a single author article.

Competing interests. The author is a shareholder in Voxalytic GmbH, a company producing microscale NMR equipment.

365 *Acknowledgements.* I would like to thank my group members for providing valuable feedback on the text.



References

- Abragam, A. and Goldman, M.: Principles of dynamic nuclear polarisation, *Reports on Progress in Physics*, 41, 395–467, <https://doi.org/10.1088/0034-4885/41/3/002>, 1978.
- Ackerman, J. L., Eckman, R., and Pines, A.: Experimental results on deuterium NMR in the solid state by magic angle sample spinning, *Chemical Physics*, [https://doi.org/10.1016/0301-0104\(79\)80092-0](https://doi.org/10.1016/0301-0104(79)80092-0), 1979.
- Adhikari, S., Wallrabe, U., Badilita, V., and Jan G. Korvink: On-chip capacitors for MACS NMR detectors, in: *Euromar 2017*, Warsaw, Poland, https://www.euromar2017.org/files/UserFiles/Euromar_2017_abstracts.pdf, 2017.
- Andreas, L. B., Jaudzems, K., Stanek, J., Lalli, D., Bertarello, A., Le Marchand, T., Cala-De Paepe, D., Kotelovica, S., Akopjana, I., Knott, B., Wegner, S., Engelke, F., Lesage, A., Emsley, L., Tars, K., Herrmann, T., and Pintacuda, G.: Structure of fully protonated proteins by proton-detected magic-angle spinning NMR, *Proceedings of the National Academy of Sciences of the United States of America*, 113, 9187–9192, <https://doi.org/10.1073/pnas.1602248113>, 2016.
- Andrew, E. R., Bradbury, A., and Eades, R. G.: Nuclear Magnetic Resonance Spectra from a Crystal rotated at High Speed, *Nature*, 182, 1659–1659, <https://doi.org/10.1038/1821659a0>, 1958.
- Andrew, E. R., Farnell, L. F., Firth, M., and Gledhill, T. D.: High-speed rotors for nuclear magnetic resonance studies on solids, *Journal of Magnetic Resonance*, 1, 27–34, [https://doi.org/10.1016/0022-2364\(69\)90004-3](https://doi.org/10.1016/0022-2364(69)90004-3), 1969.
- Arita, Y., Mazilu, M., and Dholakia, K.: Laser-induced rotation and cooling of a trapped microgyroscope in vacuum, *Nature Communications*, 4, 117, <https://doi.org/10.1038/ncomms3374>, 2013.
- Badilita, V., Fassbender, B., Kratt, K., Wong, A., Bonhomme, C., Sakellariou, D., Jan G. Korvink, and Wallrabe, U.: Microfabricated Inserts for Magic Angle Coil Spinning (MACS) Wireless NMR Spectroscopy, *PLoS ONE*, 7, e42848, <https://doi.org/10.1371/journal.pone.0042848>, 2012a.
- Badilita, V., Meier, R. C., Spengler, N., Wallrabe, U., Utz, M., and Jan G. Korvink: Microscale nuclear magnetic resonance: a tool for soft matter research, *Soft Matter*, pp. –, <https://doi.org/10.1039/C2SM26065D>, 2012b.
- Bahl, G., Tomes, M., Marquardt, F., and Carmon, T.: Observation of spontaneous Brillouin cooling, *Nature Physics*, 8, 203–207, <https://doi.org/10.1038/nphys2206>, 2012.
- Balimann, G., Burgess, M., Harris, R. K., and Oliver, A. G.: A magic-angle rotor for NMR using a forced gas bearing, *Chemical Physics*, 46, 469–475, [https://doi.org/10.1016/0301-0104\(80\)85222-0](https://doi.org/10.1016/0301-0104(80)85222-0), 1980.
- Barnes, A. B., De Paëpe, G., van der Wel, P. C. A., Hu, K. N., Joo, C. G., Bajaj, V. S., Mak-Jurkauskas, M. L., Sirigiri, J. R., Herzfeld, J., Temkin, R. J., and Griffin, R. G.: High-Field Dynamic Nuclear Polarization for Solid and Solution Biological NMR, *Applied Magnetic Resonance*, 34, 237–263, <https://doi.org/10.1007/s00723-008-0129-1>, 2008.
- Bart, J., Janssen, J. W. G., van Bentum, P. J. M., Kentgens, A. P. M., and Gardeniers, J. G. E.: Optimization of stripline-based microfluidic chips for high-resolution NMR, *Journal of Magnetic Resonance* (1969), 201, 175–185, <https://doi.org/10.1016/j.jmr.2009.09.007>, 2009.
- Bauer, J., Schroer, A., Schwaiger, R., and Kraft, O.: Approaching theoretical strength in glassy carbon nanolattices, *Nature Materials*, 15, 438–443, <https://doi.org/10.1038/nmat4561>, 2016.
- Böckmann, A., Ernst, M., and Meier, B. H.: Spinning proteins, the faster, the better?, *Journal of Magnetic Resonance* (1969), 253, 71–79, <https://doi.org/10.1016/j.jmr.2015.01.012>, 2015.
- Büttgenbach, S.: Electromagnetic Micromotors—Design, Fabrication and Applications, *Micromachines*, 5, 929–942, <https://doi.org/10.3390/mi5040929>, 2014.



- Chan, J., Alegre, T. P. M., Safavi-Naeini, A. H., Hill, J. T., Krause, A., Gröblacher, S., Aspelmeyer, M., and Painter, O.: Laser cooling of a nanomechanical oscillator into its quantum ground state, *Nature*, 478, 89–92, <https://doi.org/10.1038/nature10461>, 2011.
- 405 Ciobanu, L. and Pennington, C.: 3D micron-scale MRI of single biological cells, *Solid State Nuclear Magnetic Resonance*, 25, 138–141, <https://doi.org/10.1016/j.ssnmr.2003.03.008>, 2004.
- Deng, Y. and Korvink, J.: Topology optimization for three-dimensional electromagnetic waves using an edge element-based finite-element method, *Proceedings of the Royal Society of London. Series A*, 472, 20150 835, <https://doi.org/10.1098/rspa.2015.0835>, 2016a.
- Deng, Y. and Korvink, J.: Self-consistent adjoint analysis for topology optimization of electromagnetic waves, *Proceedings of the Royal*
 410 *Society of London. Series A*, 472, 20150 835, <https://doi.org/10.1098/rspa.2015.0835>, 2016b.
- Deschamps, M.: Ultrafast magic angle spinning nuclear magnetic resonance, *Annu Rep NMR Spectrosc*, 81, 109–144, <https://doi.org/10.1002/chin.201428297>, 2014.
- Deubel, M., von Freymann, G., Wegener, M., Pereira, S., Busch, K., and Soukoulis, C. M.: Direct laser writing of three-dimensional photonic-crystal templates for telecommunications : Article : *Nature Materials*, *Nature Materials*, 3, 444–447, <https://doi.org/10.1038/nmat1155>,
 415 2004.
- Diedrich, F., Bergquist, J. C., Itano, W. M., and Wineland, D. J.: Laser Cooling to the Zero-Point Energy of Motion, *Physical review letters*, 62, 403–406, <https://doi.org/10.1103/PhysRevLett.62.403>, 1989.
- Eckman, R., Alla, M., and Pines, A.: Deuterium NMR in solids with a cylindrical magic angle sample spinner, *Journal of Magnetic Resonance* (1969), 41, 440–446, [https://doi.org/10.1016/0022-2364\(80\)90301-7](https://doi.org/10.1016/0022-2364(80)90301-7), 1980.
- 420 Epstein, R. I., Buchwald, M. I., Edwards, B. C., and Gosnell, T. R.: Observation of laser-induced fluorescent cooling of a solid, *Nature*, pp. 500–503, <https://doi.org/10.1038/377500a0>, 1995.
- Erickson, H. P.: Size and Shape of Protein Molecules at the Nanometer Level Determined by Sedimentation, Gel Filtration, and Electron Microscopy, *Biological Procedures Online*, 11, 32, <https://doi.org/10.1007/s12575-009-9008-x>, 2009.
- Geropp, D.: Der turbulente Wärmeübergang am rotierenden Zylinder, *Ingenieur-Archiv*, 38, 195–203, <https://doi.org/10.1007/BF00536164>.
- 425 Gissibl, T., Thiele, S., Herkommer, A., and Giessen, H.: Sub-micrometre accurate free-form optics by three-dimensional printing on single-mode fibres, *Nature Communications*, 7, 11 763–, <https://doi.org/10.1038/ncomms11763>, 2016.
- Harter, T., Muehlbrandt, S., Ummethala, S., Schmid, A., Bacher, A., Hahn, L., Kohl, M., Freude, W., and Koos, C.: Silicon-plasmonic photomixer for generation and homodyne reception of continuous-wave THz radiation, in: 2016 Conference on Lasers and Electro-Optics (CLEO), pp. 1–2, IEEE, <http://ieeexplore.ieee.org/stamp/stamp.jsp?arnumber=7788747>, 2016.
- 430 Kampmann, R., Sinzinger, S., and Korvink, J. G.: Optical tweezers for trapping in a microfluidic environment, *Applied Optics*, 57, 5733–5742, 2018.
- King, J. P., Jeong, K., Vassiliou, C. C., Shin, C. S., Page, R. H., Avalos, C. E., Wang, H.-J., and Pines, A.: Room-temperature in situ nuclear spin hyperpolarization from optically pumped nitrogen vacancy centres in diamond, *Nature Communications*, 6, 8965, <https://doi.org/10.1038/ncomms9965>, 2015.
- 435 Kiss, S., MacKinnon, N., and Korvink, J.: Microfluidic Overhauser DNP chip for signal-enhanced compact NMR, *Scientific Reports*, 11, <https://doi.org/10.1038/s41598-021-83625-y>, cited By 9, 2021.
- Lowe, I. J.: Free induction decays of rotating solids, *Physical review letters*, 2, 285–287, <https://doi.org/10.1103/PhysRevLett.2.285>, 1959.
- Maricq, M. M. and Waugh, J. S.: NMR in rotating solids, *The Journal of Chemical Physics*, 70, 3300–3316, <https://doi.org/10.1063/1.437915>, 1979.



- 440 Maxon: The ultra-fast brushless DC motor, <https://www.maxonmotorusa.com/maxon/view/content/ecx-detailsite>, accessed on 23.08.2017, 2015.
- McDermott, A.: Structure and Dynamics of Membrane Proteins by Magic Angle Spinning Solid-State NMR, *Annual Review of Biophysics*, 38, 385–403, <https://doi.org/10.1146/annurev.biophys.050708.133719>, 2009.
- Meier, T., Wang, N., Mager, D., Jan G. Korvink, Petigirard, S., and Dubrovinsky, L.: Magnetic Flux Tailoring through Lenz Lenses in Toroidal
 445 Diamond Indenter Cells: A New Pathway to High Pressure Nuclear Magnetic Resonance, *arXiv.org*, <https://arxiv.org/abs/1706.00073>, under review., 2017.
- Melikyan, A., Alloatti, L., Muslija, A., Hillerkuss, D., Schindler, CP, Li J, Palmer R, Korn, D, Muehlbrandt, S, Van Thourhout, D, Chen, B, Dinu, R, Sommer, M, Koos, C, Kohl, M, Freude, W, and Leuthold, J: High-speed plasmonic phase modulators, 8, 229–233, <https://doi.org/10.1038/NPHOTON.2014.9>, 2014.
- 450 Newscaletech: Squiggle micro motor technology, <https://www.newscaletech.com/resources/technology/squiggle-micro-motor-technology/>, accessed on 23.08.2017, 2015.
- Nishiyama, Y., Endo, Y., Nemoto, T., and Utsumi, H.: Very fast magic angle spinning 1H-14N 2D solid-state NMR: Sub-micro-liter sample data collection in a few minutes - *ScienceDirect, Journal of Magnetic Resonance*, <https://doi.org/10.1016/j.jmr.2010.10.001>, 2011.
- Nishiyama, Y., Malon, M., Gan, Z., and Endo, Y.: Proton–nitrogen-14 overtone two-dimensional correlation NMR spectroscopy of solid-sample
 455 at very fast magic angle sample spinning, *Journal of Magnetic Resonance (1969)*, 230, 160–164, <https://doi.org/10.1016/j.jmr.2013.02.015>, 2013.
- Olson, D. L., Peck, T. L., Webb, A. G., Magin, R. L., and Sweedler, J. V.: High-Resolution Microcoil 1H-NMR for Mass-Limited, Nanoliter-Volume Samples, *Science*, 270, 1967–1970, <https://doi.org/10.1126/science.270.5244.1967>, 1995.
- Oschkinat, H., Müller, T., and Dieckmann, T.: Protein Structure Determination with Three- and Four-Dimensional NMR Spectroscopy,
 460 *Angewandte Chemie International Edition in English*, 33, 277–293, <https://doi.org/10.1002/anie.199402771>, 1994.
- Padgett, M. and Bowman, R.: Tweezers with a twist, *Nature Photonics*, 5, 343–348, <https://doi.org/10.1038/nphoton.2011.81>, 2011.
- Padgett, M. J.: Orbital angular momentum 25 years on [Invited], *Optics Express*, 25, 11 265, <https://doi.org/10.1364/OE.25.011265>, 2017.
- PDB: Protein data bank, <https://www.rcsb.org/pdb>, the PDB was searched for entries, based on NMR structure elucidation, on 23.08.2017, and
 465 102 entries were found. The search was performed in response to a statement made in a talk by Loren Andreas at the ISMAR in Quebec city one month earlier., 2017.
- Pines, A., Gibby, M. G., and Waugh, J. S.: Proton-Enhanced Nuclear Induction Spectroscopy. A Method for High Resolution NMR of Dilute Spins in Solids, *The Journal of Chemical Physics*, 56, 1776–1777, <https://doi.org/10.1063/1.1677439>, 1972.
- Poletkin, K. V., Lu, Z., Moazenzadeh, A., Mariappan, S. G., Jan G. Korvink, Wallrabe, U., and Badilita, V.: Polymer Magnetic Composite Core Boosts Performance of Three-Dimensional Micromachined Inductive Contactless Suspension, *IEEE Magnetics Letters*, 7, 1–3,
 470 <https://doi.org/10.1109/LMAG.2016.2612181>, 2016.
- Poletkin, K. V., Lu, Z., wallrabe, U., Jan G. Korvink, and Badilita, V.: Stable dynamics of micro-machined inductive contactless suspensions, *International Journal of Mechanical Sciences*, <https://doi.org/10.1016/j.ijmecsci.2017.08.016>, in press., 2017.
- Pringsheim, P.: Zwei Bemerkungen über den unterschied von Lumineszenz- und Temperaturstrahlung, *Z. Phys.*, 57, 739–746, <https://doi.org/10.1007/BF01340652>, 1929.
- 475 Samoson, A., Tuherm, T., Past, J., Reinhold, A., Anupöld, T., and Heinmaa, I.: New Horizons for Magic-Angle Spinning NMR, vol. 246, Springer Berlin Heidelberg, Berlin, Heidelberg, <https://doi.org/10.1007/b98647>, 2004.



- Schledorn, M., Malär, A. A., Torosyan, A., Penzel, S., Klose, D., Oss, A., Org, M.-L., Wang, S., Lecoq, L., Cadalbert, R., Samoson, A., Böckmann, A., and Meier, B. H.: Protein NMR Spectroscopy at 150 kHz Magic-Angle Spinning Continues To Improve Resolution and Mass Sensitivity, 21, 2540–2548, 2020.
- 480 Sharma, S., Rostas, A. M., Bordonali, L., MacKinnon, N., Weber, S., and Jan G. Korvink: Micro and nano patternable magnetic carbon, Journal of Applied Physics, 120, 235 107, <https://doi.org/10.1063/1.4972476>, 2016.
- Spengler, N., Höfflin, J., Moazenzadeh, A., Mager, D., MacKinnon, N., Badilita, V., Wallrabe, U., and Jan G. Korvink: Heteronuclear Micro-Helmholtz Coil Facilitates μm -Range Spatial and Sub-Hz Spectral Resolution NMR of nL-Volume Samples on Customisable Microfluidic Chips, PLoS ONE, 11, e0146384, <https://doi.org/10.1371/journal.pone.0146384>, 2016.
- 485 Spengler, N., While, P. T., Meissner, M. V., Wallrabe, U., and Jan G. Korvink: Magnetic Lenz lenses improve the limit-of-detection in nuclear magnetic resonance, PLoS ONE, 12, e0182779, <https://doi.org/10.1371/journal.pone.0182779>, 2017.
- Stepanov, V., Cho, F. H., Abeywardana, C., and Takahashi, S.: High-frequency and high-field optically detected magnetic resonance of nitrogen- vacancy centers in diamond, Applied Physics Letters, 106, 063 111, <https://doi.org/10.1063/1.4908528>, 2015.
- Tang, W. and Wang, W.: A single-board NMR spectrometer based on a software defined radio architecture, Measurement Science and Technology, 22, 015 902, <https://doi.org/10.1088/0957-0233/22/1/015902>, 2011.
- 490 Wang, N., Meissner, M. V., MacKinnon, N., Luchnikov, V., Mager, D., and Jan G. Korvink: Fast Prototyping of Microtubes with embedded sensing elements made possible with an inkjet printing and rolling process, Journal of micromechanics and microengineering, <https://doi.org/10.1088/1361-6439/aa7a61>, 2017.
- Wilhelm, D., Pürea, A., and Engelke, F.: Fluid flow dynamics in MAS systems, Journal of Magnetic Resonance (1969), 257, 51–63, <https://doi.org/10.1016/j.jmr.2015.05.006>, 2015.
- 495 Yong-Chun, L., Yu-Wen, H., and Wei, W. C.: Review of cavity optomechanical cooling, Chinese Physics B, p. 114213, <https://doi.org/10.1088/1674-1056/22/11/114213>, 2013.
- Zhang, W., Meng, G., and Li, H.: Electrostatic micromotor and its reliability, Microelectronics Reliability, 45, 1230–1242, <https://doi.org/10.1016/j.microrel.2004.12.017>, 2005.